APPLIED AND ENVIRONMENTAL MICROBIOLOGY, July 1983, p. 264–278
0099-2240/83/070264-15$02.00/0

Vol. 46, No. 1

Ethanol Production by *Saccharomyces cerevisiae* Immobilized in Hollow-Fiber Membrane Bioreactors

DOUGLAS S. INLOES,[1]† DEAN P. TAYLOR,[2]‡ STANLEY N. COHEN,[2] ALAN S. MICHAELS,[1]§ AND CHANNING R. ROBERTSON[1]*

Departments of Chemical Engineering[1] and Genetics,[2] Stanford University, Stanford, California 94305

Received 11 April 1983/Accepted 25 April 1983

Saccharomyces cerevisiae ATCC 4126 was grown within the macroporous matrix of asymmetric-walled polysulfone hollow-fiber membranes and on the exterior surfaces of isotropic-walled polypropylene hollow-fiber membranes. Nutrients were supplied and products were removed by single-pass perfusion of the fiber lumens. Growth of yeast cells within the macrovoids of the asymmetric-walled membranes attained densities of greater than 10^{10} cells per ml and in some regions accounted for nearly 100% of the available macrovoid volume, forming a tissue-like mass. A radial distribution of cell packing existed across the fiber wall, indicating an inadequate glucose supply to cells located beyond 100 μm from the lumen surface. By comparison, yeast cell growth on the exterior surfaces of the isotropic-walled membranes resulted in an average density of 3.5×10^9 viable cells per ml. Ethanol production by reactors containing isotropic polypropylene fibers reached a maximum value of 26 g/liter-h based on the total reactor volume. Reactor performance depended on the fiber packing density and on the glucose medium flow rate and was limited by low nutrient and product transport rates. The inhibition of ethanol production and the reduction in fermentation efficiency arose primarily from the accumulation of CO_2 gas within the sealed reactor shell space.

The development of large-scale, continuous microbial reactors has been limited to a major extent by an inability to maintain stable and viable cell cultures for significant periods of time. Recently, techniques for immobilizing cells on or within a solid support have attracted increasing attention for possible use in biochemical reactors (1, 4, 6, 15). These procedures frequently improve catalyst stability, and the immobilized cells can be concentrated to higher densities within the immobilization support than is possible in normal suspension cultures, resulting in potentially high reactor productivities. Moreover, the immobilization support often can be formed into geometries that provide improved mass transfer characteristics within the microbial reactor, thus increasing the efficiency of nutrient supply and product removal throughout the cell mass. One particularly attractive geometry is the cylindrical configuration provided by hollow-fiber membranes. In general, the fiber wall structure of these particular membranes possesses either an asymmetric or an isotropic morphology. Asymmetric membranes (Fig. 1) are anisotropic structures consisting of an ultramicroporous inner wall surrounded by an open-celled macroporous polymer matrix. Although originally developed for ultra-filtration applications, these fibers have been used both as solid supports for culturing mammalian tissue cells (7, 19, 29, 36) and as matrices for entrapping solutions of purified single enzymes (33). Isotropic membranes (Fig. 2) have walls with a uniform microporous structure throughout. Enzymes (10) and heat-treated *Pseudomonas fluorescens* (17) have been immobilized within reactors containing such fibers.

More recent work employing *Escherichia coli* immobilized in the macroporous walls of asymmetric hollow-fiber membranes (D. S. Inloes, W. J. Smith, D. P. Taylor, S. N. Cohen, A. S. Michaels, and C. R. Robertson, Biotechnol. Bioeng., in press) has shown that extremely high, tissue-like densities of ca. 10^{12} cells per ml are possible in such systems and that protein synthesis continues at high levels for more than 3 weeks. The primary objective of this study was to extend the previous work with bacteria to eucaryotic microorgansims by characterizing the growth of *Saccharomyces cerevisiae* ATCC

† Present address: Corporate Research and Development, Monsanto Co., St. Louis, MO 63167.
‡ Present address: Department of Molecular Genetics, Smith Kline & French Laboratories, Philadelphia, PA 19101.
§ Present address: Department of Chemical Engineering, Massachusetts Institute of Technology, Cambridge, MA 02139, and Department of Chemical Engineering, Lehigh University, Bethlehem, PA 18015.

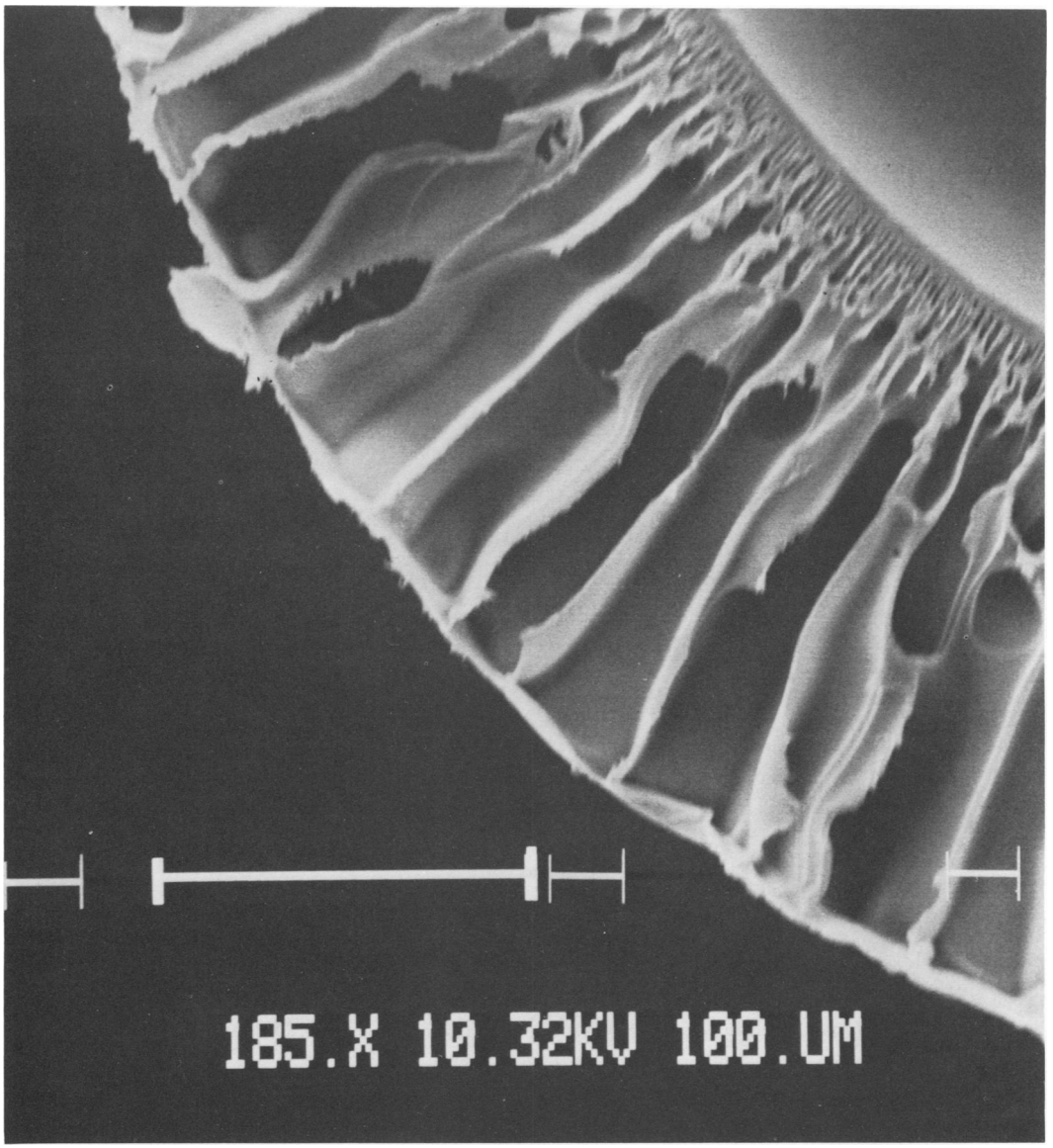

FIG. 1. Scanning electron micrograph of the macroporous wall structure of an asymmetric polysulfone hollow-fiber membrane (bar = 100 μm).

4126 and the ethanol production from glucose by *S. cerevisiae* immobilized in hollow-fiber membrane reactors. This fermentation was studied as a model metabolic system since this pathway requires either stability or continued synthesis of the associated enzymes and regeneration of the cofactor NAD or both. Electron microscopy was used to measure cell densities and to assess the cellular morphology.

MATERIALS AND METHODS

This study was divided into two sections. Initial experiments were used to examine the growth and immobilization characteristics of *S. cerevisiae* ATCC 4126 within the macroporous walls of asymmetric hollow fibers (reactor I) and on the exterior surfaces of isotropic hollow fibers (reactor II). After these experiments, ethanol production by immobilized yeast cells was studied with isotropic hollow-fiber membrane bioreactors (reactors C-20 and C-40).

Reactor design and operation. The general reactor design (Fig. 3) consisted of fibers coated with Amicon T-674 epoxy at both ends inside a 25-cm-long glass shell having two side ports. Reactor I (shell with 7-mm inside diameter [ID]) contained 20 asymmetric polysulfone fibers (Amicon Corp., Lexington, Mass.; 470-μm ID by 870-μm outer diameter [OD]) with a nominal

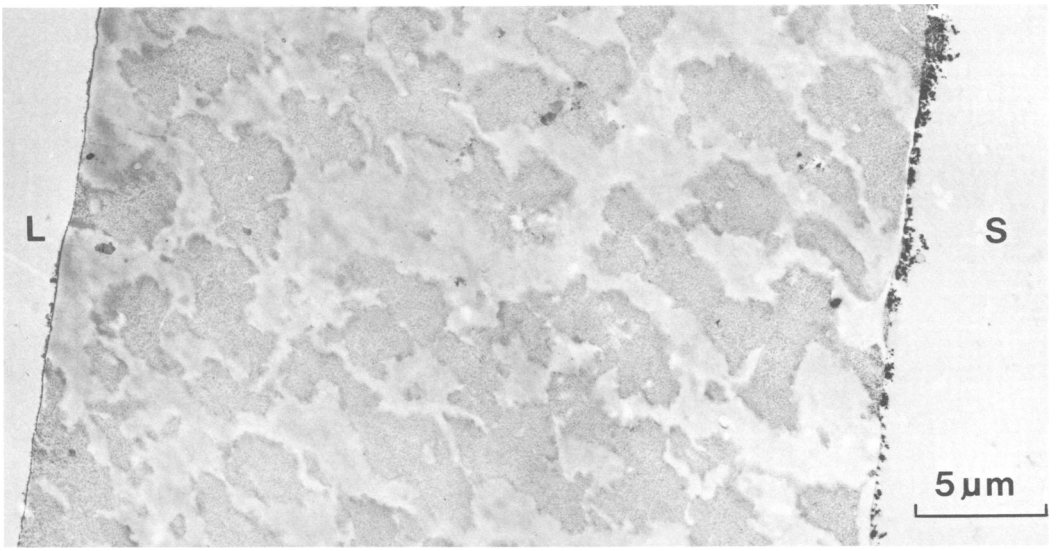

FIG. 2. Wall cross-section of an isotropic microporous polypropylene hollow-fiber membrane. L, Fiber lumen; S, shell space.

molecular weight cutoff of 10,000. Reactor II (3-mm ID shell) contained four isotropic, microporous polypropylene fibers (Celanese Corp., Charlotte, N.C.; 380-µm ID by 440-µm OD). Reactors C-20 and C-40 (5-mm-ID shell) contained 20 and 40 Celanese microporous polypropylene fibers, respectively. After the epoxy was allowed to cure, the fibers and epoxy that extended from each end of the reactor were severed, leaving the reactor ends sealed except for the fiber lumens. The remaining fiber length accessible to the cells between the ends treated with epoxy was ca. 18 cm. The fibers were wetted by ultrafiltering ca. 100 ml of distilled water across the membranes. To facilitate wetting, the polysulfone membranes were stored in 20% glycerol before use, whereas the polypropylene fibers were made permeable to water by rinsing with 50% (vol/vol) ethanol. The wetted fibers were pressurized on the lumen side with helium gas to 10 lb/in^2 to detect membrane defects of ca. 1 µm or greater. Only reactors free of membrane defects, as determined by the helium bubble point leak test, were sterilized in a 12% ethylene oxide gas mixture for 2 h at 60°C before inoculation with yeast cells. For the experiments, a sterilized reactor was placed inside an incubator maintained at a constant temperature of 35°C. Air was filter sterilized and humidified before passing through the reactor shell, and nutrient medium saturated with air was pumped continuously through the reactor lumen. Liquid samples of both the lumen effluent and the shell effluent were collected aseptically into glass tubes, and pressures for the lumen inlet, lumen outlet, and shell space were measured with manometers.

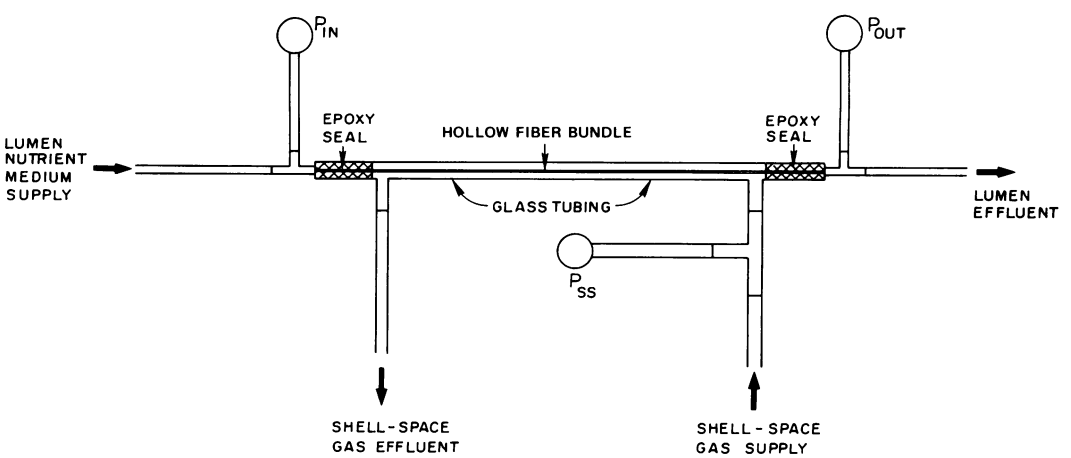

FIG. 3. Hollow-fiber reactor with connections. P_{IN}, P_{OUT}, and P_{SS} are the lumen inlet, lumen outlet, and shell space pressures, respectively.

TABLE 1. Reactor operating variables

Reactor	Hollow-fiber membrane			Nutrient medium	
	Structure	Composition	No. of fibers	Flow rate (ml/h)	Glucose concn (%, wt/vol)
I	Asymmetric	Polysulfone	20	13	1.0
II	Isotropic	Polypropylene	4	7	1.0
C-20	Isotropic	Polypropylene	20	7.4	8.9
C-40	Isotropic	Polypropylene	40	7.6	8.9

Nutrient medium was similar to that employed by Cysewski and Wilke (8) and contained the following (grams per liter of distilled water): yeast extract, 8.5; NH_4Cl, 1.32; $CaCl_2$, 0.06; and $MgSO_4 \cdot 7H_2O$, 0.11. The final glucose concentration was either 1.0% (wt/vol) (reactors I and II) or 8.9% (wt/vol) (reactors C-20 and C-40). The nutrient medium was left unbuffered at a pH of 6.2. Sterilization was accomplished by filtration through a 0.22-μm membrane filter (Millipore Corp., Bedford, Mass.). Nutrient medium flow rates were 13 and 7 ml/h for reactors I and II, respectively. Reactors C-20 and C-40 were perfused with medium at ca. 7.5 ml/h.

Immobilized yeast cell density and morphological characteristics. An exponential-phase yeast inoculum (10^7 cells per ml) was injected into the shells of reactors I and II. For reactor I, the remaining inoculum fluid was removed from the shell 6 h after inoculation, and sterile humidified air was continuously circulated through the shell at ca. 10 ml/min. To ensure that an adequate cell layer accumulated on the external surfaces of the isotropic fibers, the shell air circulation for reactor II was not initiated until 36 h after inoculation. Samples of the reactor effluent were periodically collected and plated on 1.5% (wt/vol) agar containing 1% (wt/vol) glucose medium. Reactors were operated continuously until yeast cells were detected in the reactor effluent by plating. Once this occurred, the reactors were dismantled and segments of the fibers were placed in fixative and prepared for a microscopic examination of the cell packing characteristics and cellular morphology. Fiber segments 1 cm in length were fixed for 12 to 24 h with a 3% glutaraldehyde–3% paraformaldehyde solution in 0.1 M phosphate buffer (pH 7.0), postfixed for 2 h with 1% osmium tetroxide in 0.5 M phosphate buffer, and stained for 1 h in an aqueous solution of 1% uranyl acetate. Stained sections were dehydrated in a series of progressively more concentrated ethanol solutions—5 min each in 50, 70, and 95% ethanol and 15 min (two times) in absolute ethanol. After dehydration, samples were embedded in an epoxy resin medium according to Spurr (28). Thin sections (60 to 90 nm thick) were stained with Reynolds lead citrate stain (25) and examined in a transmission electron microscope (Hitachi Hu-11E-1). With a two-dimensional grid, yeast cell densities in the macroporous walls of the asymmetric fibers were determined from electron micrographs by point-counting volumetry (Inloes et al., in press). The average volume of an immobilized cell was calculated from the average cell radius measured in the electron micrographs, assuming a spherical shape.

Ethanol production in isotropic hollow-fiber membrane bioreactors. The reactor shells of C-20 and C-40 were inoculated simultaneously with an exponential-phase yeast inoculum (10^7 cells per ml). The inoculum was not drained from the reactor shell, and both shell ports of each reactor were closed for the duration of the experiment so that nutrients and products could leave the reactor only by way of the fiber lumens. Samples of the reactor effluent were periodically collected on ice and plated to check for contamination. For ethanol and glucose determinations, 0.1 ml of 33 mM sodium azide was added to 1.0 ml of collected sample, which was stored in a capped vial at 3°C until assayed. The effluent flow rate was measured. Ethanol concentrations were determined by alcohol dehydrogenase assay (Sigma Chemical Co. technical bulletin no. 331-UV, St. Louis, Mo.); glucose concentrations were measured by hexokinase plus glucose 6-phosphate dehydrogenase assay (Sigma Chemical Co. technical bulletin no. 15-UV).

Table 1 summarizes the variables for each of the four reactors tested.

RESULTS

Immobilized yeast cell density and morphological characteristics. Fiber sections taken from reactor I after 3.3 days of culture were examined by electron microscopy to determine the packing characteristics of the immobilized yeast cells. The cells were found to be nonuniformly distributed among different fibers in the bundle. In 40% of the fibers examined, yeast cells were randomly and sparsely distributed in less than half of the wall macrovoids. In these fibers, a wide spectrum of cell types was observed, ranging from cells having a normal appearance to cells containing large vacuoles. Intracellular degradation of the cytoplasmic ribosomes was also observed in some yeasts. In the remaining 60% of the fibers, yeast cells filled available wall macrovoids to high densities. A radial distribution of cells was observed in which the most dense packing occurred near the lumen surface (Fig. 4A). In these fibers, yeast cells generally accounted for 70 to 100% of the accessible void volume within 100 μm of the lumen, achieving an average cell density of 1.3×10^{10} cells per ml. By comparison, in the outer 100 μm of these same fibers (Fig. 4B), cell packing was only between 35 and 55% of the accessible void volume, and the cell density averaged 7×10^9 cells per ml. Sections taken from the inlet and

outlet ends of the reactor showed similar packing characteristics; therefore, it is unlikely that an axial distribution of cell packing existed along individual fibers of the reactor bundle.

In the densely packed fibers, yeast cells within 100 μm of the lumen grew to higher densities, were generally larger, and displayed different morphological characteristics than did cells located near the outer wall. Cells near the lumen underwent considerable distortion of shape (Fig. 5), evidently from forces generated by the actively growing cell mass. Numerous small lipid droplets also accumulated within the cytoplasm of most cells, and the degree of cytoplasmic staining varied among cells. This variability in cytoplasmic staining appeared to be random, indicative of a random distribution of cell states and not an artifact of the specimen preparation. The nature of this staining difference remains unexplained. The nuclear and vacuolar membranes within yeast cells near the fiber lumen were intact (Fig. 6), and segments of the endoplasmic reticulum were apparent. Double-membrane mitochondrial profiles possessing nondistinct cristae, typical of anaerobic or glucose-repressed cells (16, 32), were also present. The appearance of these cells contrasted markedly with that of the yeast cells located in the outer 100 μm of the fiber wall (Fig. 7). The yeast cells within this outer region possessed extremely large vacuoles and even showed signs of autolysis. Cytoplasmic staining was very dark and revealed no discrete ribosomes and very little inner detail, and the lipid content was considerably less than for cells located near the lumen.

The packing behavior for yeast cells immobilized in reactor II differed from that observed in asymmetric membranes. Instead of growing to a high density within the fiber wall, cells grew on the fiber surfaces in a very thick and viscous layer that spread throughout the interfiber spaces. After 28 days of culture, a viable cell density of 3.5×10^9 cells per ml was measured for the cell suspension collected from the reactor shell. This density corresponds to 23% of the suspension volume being occupied by viable cells. During fixation, however, the yeast cells were flushed from the fiber surface, making it impossible to obtain suitable thin sections of the immobilized cells for electron microscopy. Consequently, it was not possible to assess cellular morphology as a function of radial distance from the fiber surface for reactor II.

Cell growth within the relatively confined macrovoids of the asymmetric-walled membrane contributed to loss of membrane integrity, as evidenced by the appearance of yeast cells in the lumen effluent after 2 days of culture. Microscopic examination of these membranes revealed holes that were either preexisting defects undetected by the helium bubble point leak test or defects created by continued cell growth in the wall macrovoids. By comparison, isotropic-walled membranes proved to be considerably more effective in preventing cell entry into the fiber lumen, remaining intact after more than 28 days of culture. The improved performance of the isotropic membranes resulted from yeast cells being unable to penetrate the microporous structure of the fiber wall (Fig. 2). It was primarily because of this improved cell containment behavior that ethanol production was studied with reactors containing isotropic hollow fibers.

Ethanol production in isotropic hollow-fiber membrane bioreactors. Within 6 h after inoculation, most of the shell space liquid in reactors C-20 and C-40 was displaced by CO_2 gas, and CO_2 bubbles appeared in the reactor effluent. A very dense and viscous cell layer accumulated on the exterior surfaces of the fibers shortly after inoculation, and this layer was thicker at the reactor inlet than at the outlet. Cell material continued to accumulate in the reactor shell until, after 4 days of culture, nearly all of the volume external to the fibers in both reactors was packed with a dense cell mass containing random CO_2-filled spaces. Carbon dioxide accumulated within the shell spaces of both reactors, as evidenced by the high shell space pressures measured. The C-40 shell space pressure increased rapidly to 250 mmHg (ca. 33.3 kPa; above atmospheric) within 3 days after inoculation and continued to increase steadily over the next 5 days to a level above 500 mmHg (ca. 66.6 kPa). This pressure was considerably higher than the average lumen pressure of 40 mmHg (ca. 5.3 kPa). The buildup of shell space pressure was significantly slower in reactor C-20, however, and it eventually stabilized at a level of 330 mmHg (ca. 44.0 kPa), after 4 days of culture. These high pressures contributed to problems in maintaining an adequate flow of glucose medium through the reactors, particularly through C-40. For example, the C-40 flow rate declined from an initial value of 7.6 to 3.0 ml/h after 8 days of culture, as the lumen pressure increased to well over 500 mmHg. The C-40 effluent remained sterile for 8 days, but samples collected after 8 days contained a high density of *S. cerevisiae*. A microscopic examination of C-40 fiber segments after 8 days revealed that several fibers were partially collapsed, most likely as a consequence of the high CO_2 pressure generated within the reactor shell. Fiber collapse may have contributed to the creation of defects in the hollow-fiber membranes. The C-20 flow rate also decreased from its original level of 7.4 to 3.1 ml/h after 8 days of culture. The C-20 lumen pressure did not increase significantly, and the reactor effluent remained free of yeast cells. After readjusting

the tension on the manifold tubing for the peristaltic pump, the C-20 flow rate returned to its original level for the remainder of the experiment. Concurrent with these flow problems at 8 days, yeast cells located near the outlet ends of both reactors became pink, whereas cells at the inlet ends remained their normal off-white color. This color change correlated with the observed reduction in flow rate, perhaps as a result of nutrient limitation.

For comparison purposes, ethanol productivities for the two reactors were evaluated using two different volume bases. In one approach, these values were expressed in terms of the total reactor volume (Fig. 8A) for a comparison with other fermentation techniques. The total reactor volume is defined as the sum of the fiber volume (based on the fiber OD) and the shell volume accessible to yeast cells between the epoxy endseals. Reactor C-40 reached a maximum productivity of 26 g/liter-h at 2 days. Ethanol productivity for reactor C-20 was less but remained more stable at ca. 17 g/liter-h. The decline in C-20 productivity observed at 8 days correlated with the aforementioned reduction in flow rate from 7.4 to 3.1 ml/h. Ethanol productivities expressed in terms of the total reactor volume, however, do not provide a suitable basis for comparing results for the two hollow-fiber reactors of this study. Both the fiber volume and the shell space volume available for yeast cell immobilization differed between the C-20 and C-40 reactors, and total reactor volume does not account for either of these effects. Since scaling up to larger dimensions involves adding more fiber volume in conjunction with appropriate changes in the reactor flow rate, these reactors were therefore compared on a basis of total fiber volume (Fig. 8B). The total fiber volume is calculated from the fiber OD and the fiber length between the epoxy endseals. On this basis, the productivity for reactor C-20 was significantly higher than that for reactor C-40 at all times. These results indicate that the addition of more fibers to the same reactor shell volume reduces the production efficiency per unit of fiber volume. This reduced efficiency may be caused by a combination of transport and kinetic limitations within the reactor.

Glucose consumption rates, based on total fiber volume, are presented for both reactors in Fig. 9. The values for reactor C-20 were higher than those for reactor C-40, following the same general behavior as the ethanol productivity (Fig. 8B). For reactor C-20, the fraction of glucose converted in this single-pass mode of operation ranged from 18 to 28% under normal flow conditions, but increased to 39% at day 8. If all of the glucose consumed by the immobilized yeast cells was fermented to ethanol and CO_2, a theoretical maximum of 2 mol of ethanol and 2 mol of CO_2 should have been formed for every mol of glucose catabolized. As a measure of the effectiveness with which this occurred, the fermentation efficiency (Fig. 10) was expressed as the ratio of the moles of ethanol actually produced to the theoretical moles of ethanol expected from the measured glucose consumption. During the first 3 days of culture, the C-40 efficiency of ca. 100% was significantly higher than the value of 75% for C-20. After 5 days of culture, however, the C-40 efficiency dropped to the same level as that for C-20. Consequently, the decline in ethanol productivity for reactor C-40 (Fig. 8B) by day 5 appeared to correlate roughly with the fermentation efficiency. For reactor C-20, the efficiency remained fairly stable throughout most of the experiment, ranging from 60 to 80%.

Attempts were also made to calculate CO_2 production rates for these reactors by measuring the flow rates for both dissolved CO_2 and CO_2 gas in the reactor effluent. Gas flow rates were determined from the known effluent tubing radius in conjunction with transit time measurements of gas slugs through a predetermined length of outlet tubing. Assuming that the liquid effluent was saturated with CO_2, the efflux rate for dissolved CO_2 was added to the gas flow rate to give the total CO_2 generation rate. Due to uncertainty in the value for the tubing radius, however, it was not possible to quantify this rate accurately. Qualitatively, the CO_2 production rate followed the same general pattern as that of the ethanol productivity for both reactors, and the molar rates of production were at least as high as the ethanol formation rates. The pH of the unbuffered glucose medium showed the effects of these high CO_2 levels, decreasing from a value of 6.2 to 4.7 in a single pass through the reactor.

DISCUSSION

One of the most significant factors limiting productivity in continuous ethanol fermentations is the quantity of catalyst available to perform the microbiological transformation. Since microbial cells are difficult to culture effectively at a high density in conventional chemostats, many different techniques have been employed in an attempt to increase the microbial population density within such fermentors. Some approaches have facilitated the continuous separation of the inhibitory metabolic products such as ethanol from the fermentation medium by either operating under vacuum conditions (9, 24) or filtering the cell suspension through a rotating microporous membrane (21). Other approaches have employed the separation of a concentrated cell suspension from the prod-

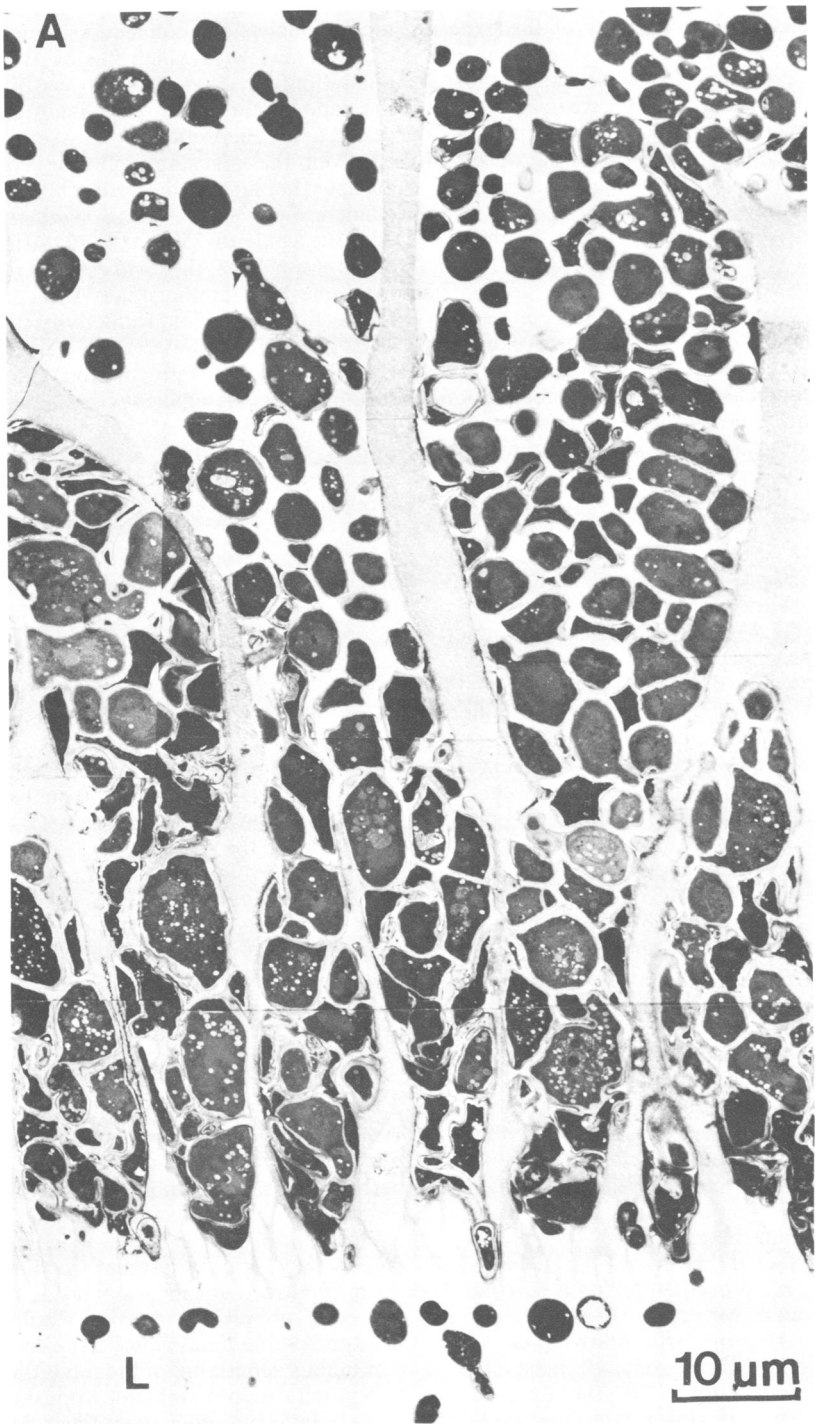

FIG. 4. Immobilized *S. cerevisiae* located (A) within 100 μm of the lumen surface (L, fiber lumen) and (B) within 100 μm of the outer fiber surface (S, shell space) in a densely packed fiber of reactor I.

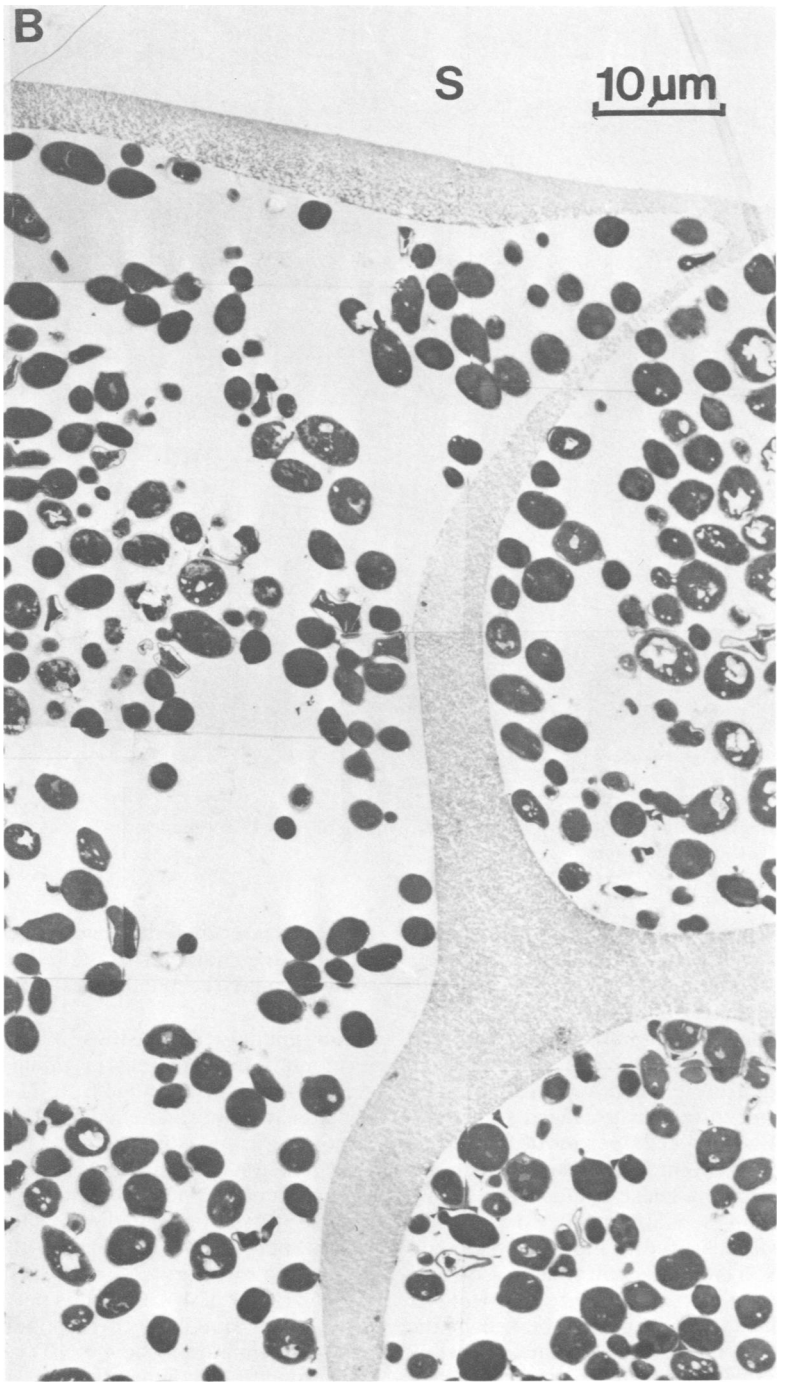

FIG. 4—*Continued*

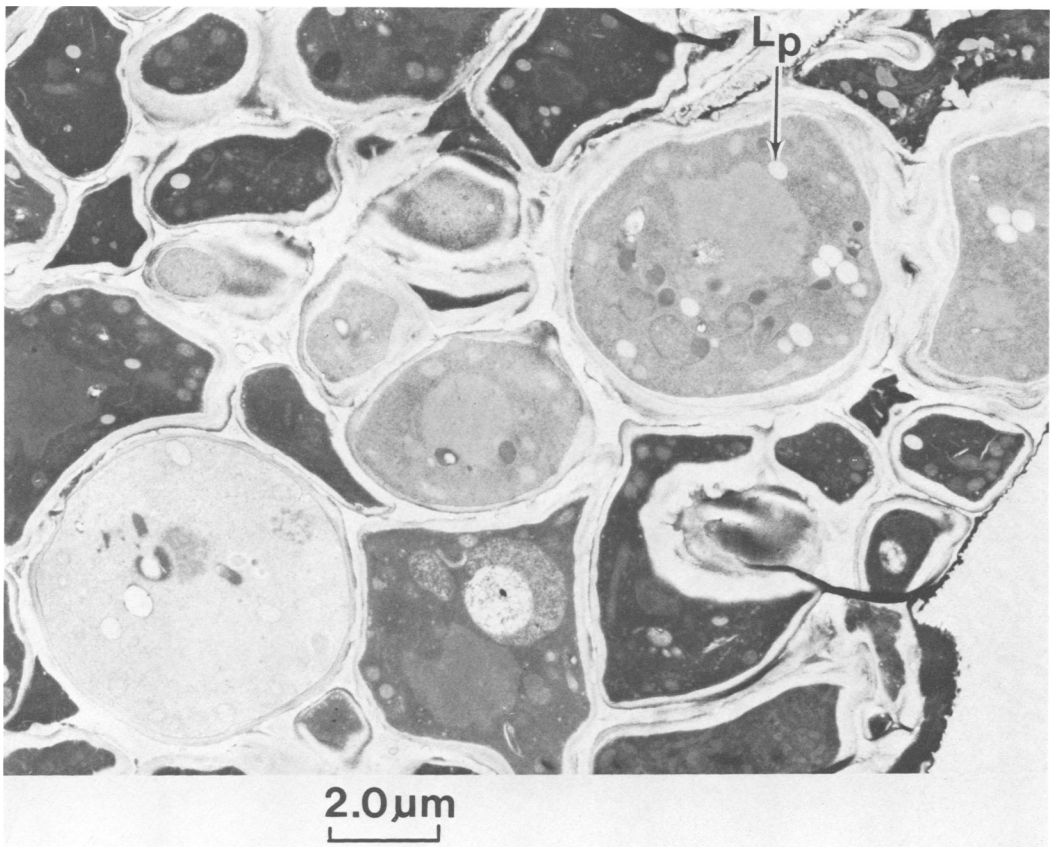

FIG. 5. Packing behavior of *S. cerevisiae* located within 100 μm of the lumen surface in a densely packed fiber of reactor I. L_P, Lipid droplet.

uct stream, using either a cell settler (9, 11) or membrane filtration (26), for subsequent recycle back to the fermentor.

The immobilization of yeast cells within the hollow-fiber reactors used in this study provided an optional method for achieving extremely high densities. In densely packed asymmetric membranes, cell concentrations averaged between 7×10^9 and 1.3×10^{10} cells per ml of accessible void volume, depending on the radial distance from the fiber lumen. These values were significantly higher than the viable cell density of 3.5×10^9 cells per ml measured in the isotropic membrane reactors. Yeast cells cultured on isotropic membranes were not exposed to the volume constraints placed on cells immobilized in the macrovoids of asymmetric membranes, possibly explaining the observed difference in cell density. In addition, cell densities measured from electron micrographs for the asymmetric membranes probably led to an overestimation of the actual number of viable immobilized cells. By increasing the packing density of isotropic fibers in the reactor shell volume and correspondingly reducing interfiber distances, a culture having cell packing characteristics similar to those seen with asymmetric membranes would be expected.

Maximum cell densities reported for other fermentation techniques in which *S. cerevisiae* ATCC 4126 is used range from 11 g (dry weight) per liter for a normal chemostat operated under atmospheric pressure (8) to 124 g (dry weight) per liter for a chemostat conducted simultaneously under vacuum conditions and a cell recycle (9). An intermediate value of 25 g (dry weight) per liter was achieved with a membrane-moderated rotorfermentor (21). Assuming a conversion factor of 4×10^{10} cells per g (dry weight) for *S. cerevisiae* (11), corresponding cell densities are estimated to be 4×10^8 cells per ml for the conventional chemostat, 1×10^9 cells per ml for the rotorfermentor, and 5×10^9 cells per ml for the vacuum chemostat. The cell suspension viscosity increases rapidly with cell density, leading to excessive power requirements for agitation in chemostat cultures. Since the ratio of the suspension viscosity to the viscosity of

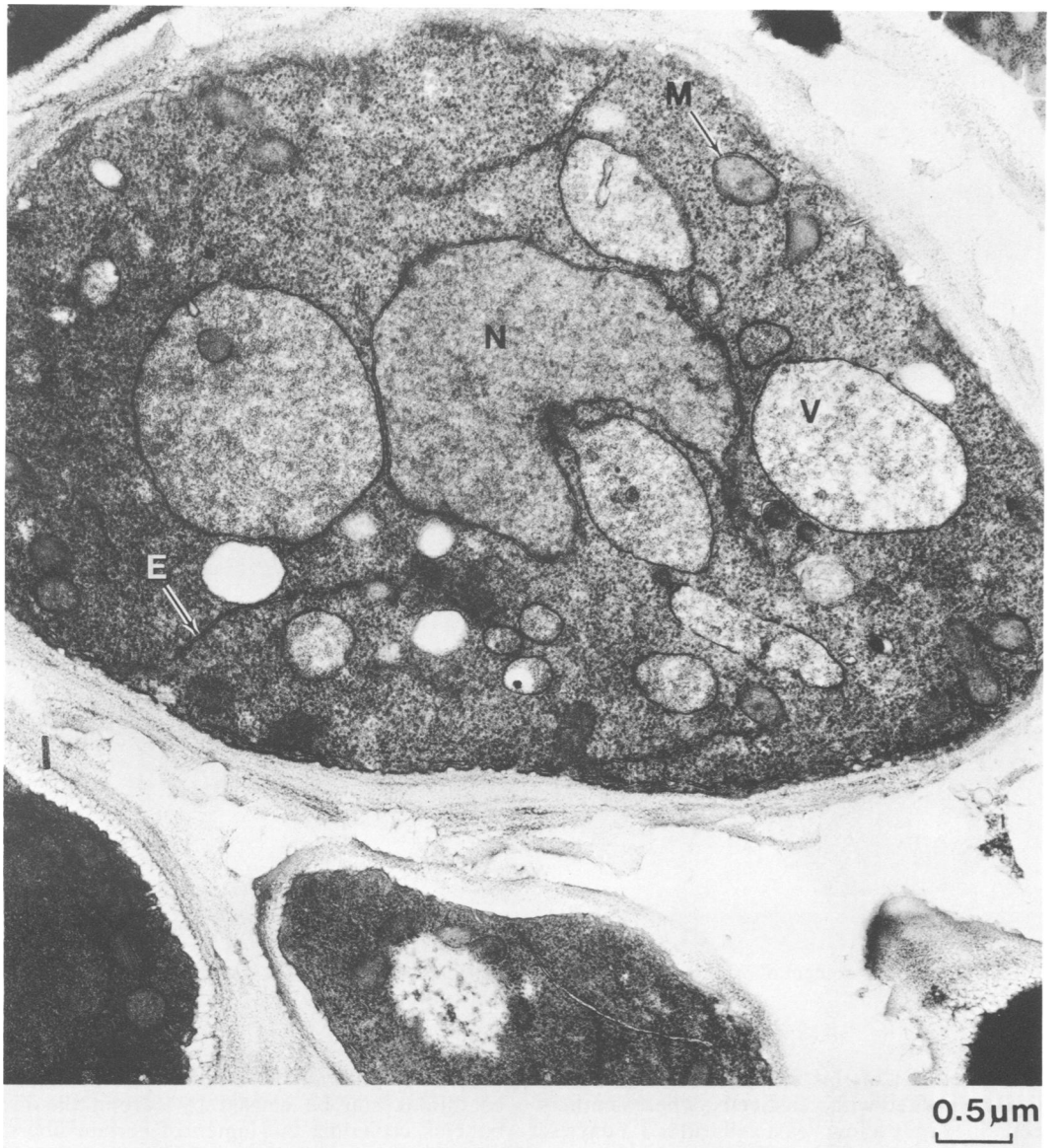

FIG. 6. Intracellular morphology of *S. cerevisiae* located within 100 μm of the lumen surface in a densely packed fiber of reactor I. E, Endoplasmic reticulum; M, mitochondrion; N, nucleus; V, vacuole.

water rises more than 2 orders of magnitude as the cell volume fraction approaches 50% (20), viscosity places an upper practical limit on the density attainable in chemostat cultures. Continuous agitation is not required in hollow-fiber membrane cultures, and immobilized cell packing has an upper bound of 100% of the accessible volume. Whole-cell immobilization also does not suffer from the problems encountered during a cell recycle, when the live cells are frequently traumatized and poorly concentrated (37). Wada et al. (31) immobilized *S. cerevisiae* in carrageenan gel beads having a mean diameter of 4 mm. This immobilization procedure retained cell viability, and a maximum density of 6.3×10^9 viable cells per ml of gel was reported. Limited transport of nutrients and products apparently restricted cell growth to only a thin, dense layer near the bead surface (30), indicating inefficient use of the void volume within the immobilization support. Although not reported, yeast cell densities in the outer regions of these beads most likely approached the high levels measured in the asymmetric membranes of this study.

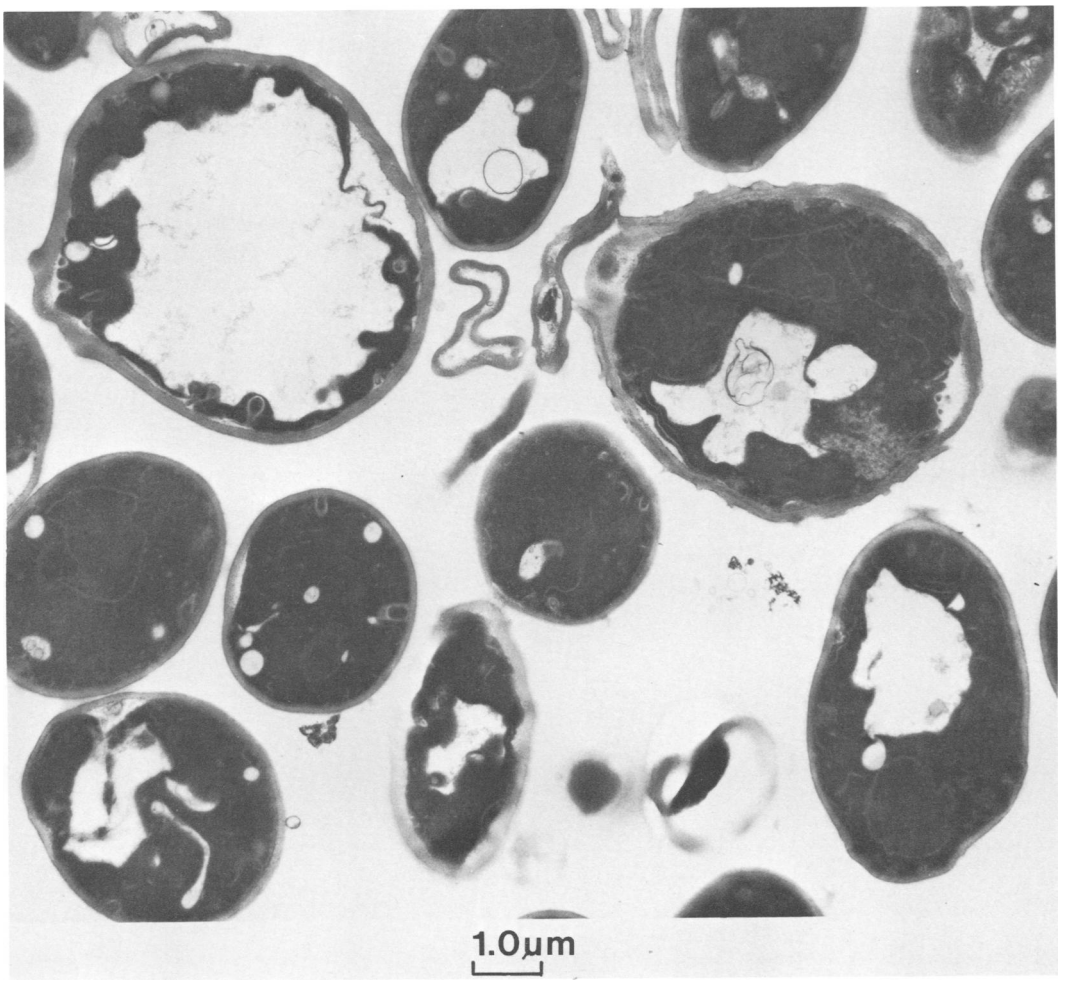

FIG. 7. Vacuole content of *S. cerevisiae* located within 100 μm of the outer fiber surface in a densely packed fiber of reactor I.

In reactor I of this study, some fibers were densely packed with yeast cells, whereas others contained only a few yeast cells after 3.3 days of culture. Two possible explanations for this nonuniform distribution of cell densities exist. Yeast cells are not motile, so cells from the inoculum may not have been able to grow into the wall macrovoids of certain fibers. Although this may have occurred in specific regions of an individual fiber, it cannot explain entire fiber lengths without cell growth, and no differences were found in the cell packing densities between the inlet and outlet ends of individual fibers. The more likely explanation is that the flow rate was not uniform throughout all fibers of the bundle and may have approached zero in some cases. Subsequent studies with multifiber reactors for ethanol production (D. S. Inloes, A. Matin, A. S. Michaels, and C. R. Robertson, manuscript in preparation) revealed that stagnant flow conditions can be caused by carbon dioxide bubbles occluding the lumen of certain fibers, which in turn would limit cell growth.

The effects of transport limitation were also apparent in outer wall regions of fibers that displayed dense cell packing (Figs. 4B and 7). Assuming that cells located in the macrovoids of the fiber wall had the same initial density as the inoculum and were growing exponentially with a growth constant of 0.45 h^{-1} (3), only 16 h would be required to achieve 100% packing of the void spaces. A one-dimensional, steady-state diffusive flux model (D. S. Inloes, Ph.D. thesis, Stanford University, Stanford, Calif., 1982) was derived for glucose transport from the fiber lumen. With a cellular glucose consumption rate of 6.2×10^{-17} mol per cell-sec (8), an effective diffusivity for glucose of 0.1×10^{-5} cm^2/s (2),

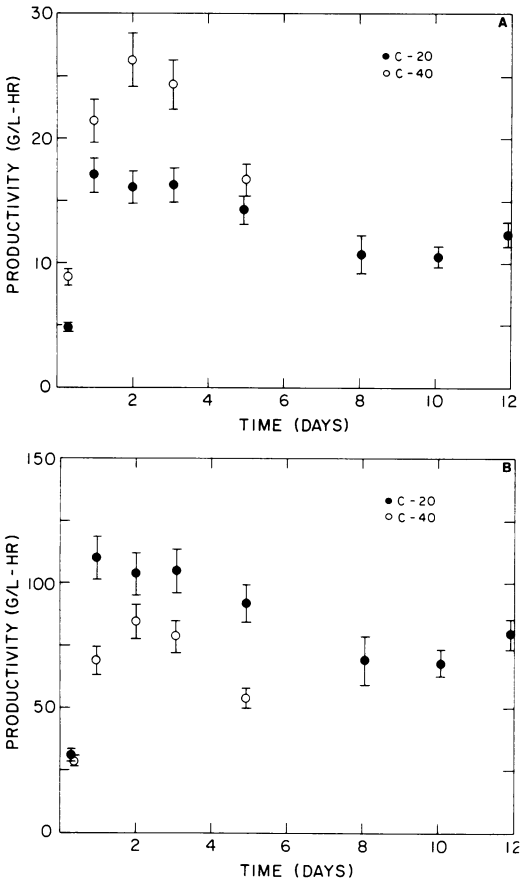

FIG. 8. Ethanol productivity (A) per total reactor volume and (B) per total fiber volume for reactors C-20 and C-40. The total reactor volume was 3.5 ml for both C-20 and C-40. The total fiber volume was 0.6 and 1.1 ml for C-20 and C-40, respectively. Error intervals represent 95% of a normal distribution centered around the mean.

and a yeast cell density of 1.5×10^{10} cells per ml, the maximum distance that glucose could be transported before it was entirely consumed was only 110 μm, which agreed with the maximum thickness of 100 μm for the densely packed cell layer seen in Fig. 4A. Increasing the glucose concentration at the lumen surface to 10% (wt/vol) would extend this distance to 350 μm, making it possible to adequately supply the entire 200-μm wall thickness. Although only glucose supply was considered here, transport of other growth factors, vitamins, or nutrients may similarly be limited.

The cellular morphologies of yeast cells located at various radial positions throughout the fiber wall were consistent with nutrient limitation. Within 100 μm of the fiber lumen (Fig. 5), cells displayed intact walls and intracellular membranes and only a minimal amount of autolysis, despite undergoing considerable deformation. A high ribosome content indicated that these cells were capable of protein synthesis. The presence of lipid droplets, an alternate form of energy storage to glycogen, indicated that these cells were not starved for glucose. These droplets are normally composed of triacylglycerols and are synthesized under conditions of excess glucose (14). Since very little cytoplasmic lipid accumulated in cells located in the outer 100 μm of the fiber wall (Fig. 7), glucose supply to these cells was possibly limited, as supported by the previous glucose transport calculations. Cells near the outer wall also possessed large electron-transparent vacuoles that are frequently indicative of a significant turnover of macromolecules, such as proteins and nucleic acids (22). When cells are challenged with starvation conditions, protein turnover rates usually increase significantly (12). The large size and relatively high frequency of these vacuoles suggest that the yeast cells in the outer wall regions were either starved for nutrients or adapting to a new environment. Similar problems of nutrient availability also apply to other fibers of the reactor bundle that were only sparsely packed with cells as a consequence of stagnant flow conditions. Evidence of ribosome degradation in cells located within these fibers indicated that these yeast cells were possibly starved for some required nutrient.

Ethanol productivities based on the total reactor volume (Fig. 8A) reached a maximum value of 26 g/liter-h for reactor C-40 and 17 g/liter-h for reactor C-20. Maximum ethanol productivities have been reported for other fermentation techniques with the same *S. cerevisiae* strain. Representative values include 7 g/liter-h for a conventional chemostat operated at atmospheric

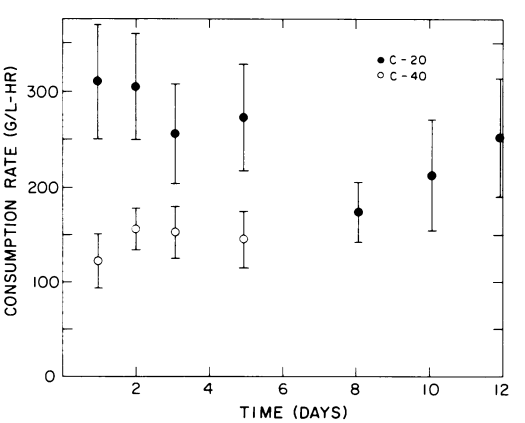

FIG. 9. Glucose consumption rate per total fiber volume for reactors C-20 and C-40.

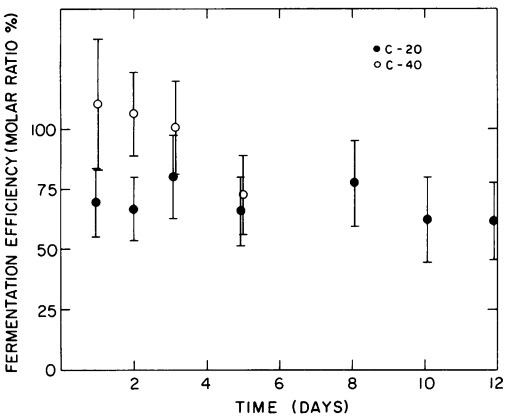

FIG. 10. Fermentation efficiency for reactors C-20 and C-40.

pressure (8), 27 g/liter-h for a membrane-moderated rotorfermentor (21), and 82 g/liter-h for a chemostat conducted simultaneously under vacuum conditions and a cell recycle (9). Using *Zymomonas mobilis*, Rogers et al. (26) reported an ethanol productivity of 120 g/liter-h for an atmospheric chemostat with a cell recycle. Various immobilized yeast cell systems have also been used for ethanol fermentation. For example, a maximum productivity of 53.8 g/liter-h has been reported for a packed column of *S. cerevisiae* immobilized within calcium alginate beads (34). Wada et al. (30) used *Saccharomyces carlsbergensis* immobilized in carrageenan gel beads to achieve an ethanol productivity of 50.0 g/liter-h of gel.

Cell densities were not measured for either reactor C-20 or reactor C-40, but assuming a uniform distribution of 3.5×10^9 cells per ml throughout the shell volume, the cellular ethanol production rates for these two reactors ranged between 6×10^{-12} and 1×10^{-11} g per cell-h. By comparison, Nagodawithana et al. (23) reported ethanol production by *S. cerevisiae* of between 3.6×10^{-12} and 5.8×10^{-11} g per cell-h for rapid batch fermentations, in agreement with a value of 5.4×10^{-11} g per cell-h for a vacuum chemostat (24). On the assumption that 1 g (dry weight) of *S. cerevisiae* ATCC 4126 contained 4×10^{10} cells, the chemostat, rotorfermentor, and vacuum chemostat described above were also estimated to have ethanol productivities of ca. 1×10^{-11} g per cell-h.

The fermentation efficiency normally lies between 90 and 95% in most chemostat applications, where most of the remaining 10% of the glucose provides precursors for the synthesis of cellular constituents. The fermentation efficiencies of the isotropic hollow-fiber reactors in this study (Fig. 10) generally varied between 60 and 80%, although the efficiency of reactor C-40 approached 100% during the first 3 days of culture. This initial difference between reactors C-20 and C-40 may have been related to the number of fibers packed into the reactor shell. Fermentation efficiencies of below 90% indicated that glucose was metabolized to form products other than ethanol, CO_2, and the normal cellular constitutents, such as lipid and glycogen. Similar fermentation efficiencies of between 65 and 90% have been reported for *S. cerevisiae* immobilized in calcium alginate beads (18) and for a vacuum fermentation with a cell recycle (24).

On a basis of total reactor volume (Fig. 8A), the C-40 ethanol productivity was significantly higher than that for reactor C-20 during the first 5 days of culture. Reactor C-40 contained twice as many fibers and possessed a smaller volume for cell immobilization than did reactor C-20. Since nutrient supply and product removal rates for the immobilized cell mass are proportional to the membrane surface area available for transport, the additional membrane area in reactor C-40 may have produced higher cell densities, resulting in a higher fermentation efficiency during the initial stages of culture (Fig. 10). On a basis of total fiber volume (Fig. 8B), however, the C-20 productivity was significantly higher and considerably more stable than the C-40 values, even though the C-20 fermentation efficiency was less. This difference in performance indicated that reactor scale-up was probably complicated by a number of different factors, including nutrient and product transport and the replacement of potential cell volume with noncatalytic fiber volume. The productivity per fiber volume may decrease as more fibers are added to a given volume. Alternatively, the higher initial production rates in reactor C-40, made possible by the greater membrane surface area, could contribute to a significant accumulation of inhibitory products if they were not removed effectively from the immobilized cell mass. In this case, the productivity would decline after reaching an initial maximum, as was observed for reactor C-40 (Fig. 8B).

Glucose transport apparently was not limiting in the C-20 and C-40 reactors. With the one-dimensional diffusion model for glucose transport and assuming an average shell space density of 3.5×10^9 cells per ml, passive diffusion is capable of transporting glucose more than 550 μm from the membrane surface into the shell space cell mass in the isotropic hollow-fiber reactors. For this calculation, the glucose concentration at the lumen surface was assumed to be the lowest measured effluent value of 6.3% (wt/vol). The arrangement of fibers was not uniform, and a few isolated regions located more

than 550 μm from the nearest fiber may have existed.

Although the glucose supply was probably adequate, the supply of other nutritents, either having a lower diffusivity or being present in lower concentrations than glucose, may have been insufficient to support high ethanol productivities. The cell packing in both reactor C-20 and reactor C-40 declined from the inlet to the outlet ends, so the flow rates used may have been sufficiently low to limit yeast cell growth. When the C-20 flow rate fell to less than one-half of its original level after 8 days of fermentation, cells near the outlet end of the reactor simultaneously became pink, compared with the normal off-white color of cells located in the inlet half of the reactor. This color change was accompanied by a significant reduction in ethanol productivity (Fig. 8B). Pink pigments normally do not occur in *S. cerevisiae*, except in certain adenine-dependent strains (22) or when the medium contains suboptimal amounts of biotin (27). No evidence has been reported to suggest that this particular yeast strain requires adenine for growth. Biotin, however, is required for the maintenance of high fermentation rates (35), so the observed decline in productivity may have been due to a biotin deficiency. A significant axial concentration gradient may exist when low flow rates are used. More uniform conditions along the entire reactor length may be achieved if the reactor effluent is recycled at a higher flow rate. Due to the higher axial pressure drop along the reactor, high recycle rates would also help to maintain a more uniform distribution of flow through all fibers of the reactor bundle.

Mass transport limitations also can influence the rates of fermentation product removal, leading to potential product inhibition effects. Such ethanol inhibition of growth rate and ethanol production has been reported for *S. cerevisiae* (8, 13). The maximum ethanol concentrations measured in the C-20 and C-40 effluents were less than 1.5% (wt/vol), well below the levels of significant inhibition. By use of a steady-state, one-dimensional diffusion analysis, and the assumption of an average cell density of 3.5×10^9 cells per ml, an ethanol diffusivity of 0.5×10^{-5} cm^2/s, and a cellular ethanol productivity of 1×10^{-11} g per cell-h (23), the maximum ethanol concentration expected in the reactor shell was less than 2% (wt/vol), indicating adequate ethanol removal for the hollow-fiber reactors.

The shell space CO_2 pressures in reactors C-20 and C-40 increased to levels above 300 mmHg (ca. 40 kPa) after 4 days of culture and thus displaced liquid from this region. Chen and Gutmanis (5) reported that *S. cerevisiae* growth was inhibited when aeration mixtures containing 50% CO_2 were used, and at 80% CO_2 the ethanol production dropped to 80% of its original level. The CO_2 pressures measured in reactors C-20 and C-40 were well above these levels, so both yeast cell growth and ethanol production were probably inhibited by CO_2. The C-40 pressure increased much more rapidly than did the C-20 pressure, which may explain the reductions in both ethanol productivity (Fig. 8B) and fermentation efficiency (Fig. 10) observed for reactor C-40 after 5 days of culture. The high CO_2 production rate also reduced the unbuffered reactor effluent pH to 4.7 from an inlet value of 6.2. Recently, a pH optimum of between 5.0 and 5.5 has been suggested for maximum ethanol productivity in this yeast strain (H. W. Blanch, personal communication). The reduction in the pH also may have contributed to the inhibition of yeast growth and ethanol productivity.

The high CO_2 pressure in reactor C-40 probably caused the eventual collapse of the hollow fibers and created defects in the isotropic membranes. Removal of CO_2 therefore becomes imperative for this reactor design. Venting the reactor shell to the atmosphere or flushing the reactor shell with air might alleviate the problem of high CO_2 pressures, but the CO_2 concentrations would still be high within the interior of a densely packed fiber bundle. Alternatively, more uniform airflow patterns might be possible if yeast cells were contained within the macroporous walls of asymmetric hollow-fiber membranes which might not require packing in tight arrays. By limiting the wall thickness of such membranes to reduce CO_2 diffusion distances, dissolved CO_2 concentrations could be maintained below saturating levels. Effective control of yeast cell growth would be necessary to minimize the accumulation of cells within the fiber lumen and the interfiber spaces.

ACKNOWLEDGMENTS

We express our sincere gratitude to Fran Thomas, Ann Yoshimura, William Smith, Chris Miller, Abdul Matin, Harvey Blanch, and Barry Solomon for their comments, suggestions, and technical assistance. The asymmetric polysulfone membranes and isotropic polypropylene membranes were kindly supplied by Amicon Corp. and Celanese Chemical Co., respectively.

This work was supported by Stanford University. D.P.T. acknowledges postdoctoral fellowship support from the Bank of America-Giannini Foundation.

LITERATURE CITED

1. **Abbott, B. J.** 1976. Preparation of pharmaceutical compounds by immobilized enzymes and cells. Adv. Appl. Microbiol. **20**:203–257.
2. **Bailey, J. E., and D. F. Ollis.** 1977. Biochemical engineering fundamentals, p. 396. McGraw-Hill Book Co., New York.
3. **Bazua, C. D., and C. R. Wilke.** 1977. Ethanol effects on the kinetics of a continuous fermentation with *Saccharomyces cerevisiae*. Biotechnol. Bioeng. Symp. **7**:105–118.
4. **Cheetham, P. S. J.** 1980. Developments in the immobilization of microbial cells and their applications, p. 189–238.

In A. Wiseman (ed.), Topics in enzyme and fermentation biotechnology, vol. 4. John Wiley & Sons, Inc., New York.
5. **Chen, S. L., and F. Gutmanis.** 1976. Carbon dioxide inhibition of yeast growth in biomass production. Biotechnol. Bioeng. **18**:1455–1462.
6. **Chibata, I., T. Tosa, and T. Sato.** 1979. Use of immobilized cell systems to prepare fine chemicals, p. 433–461. *In* H. J. Peppler and D. Perlman (ed.), Microbial technology, vol. 2, 2nd ed. Academic Press, Inc., London.
7. **Chick, W. L., A. A. Like, V. Lauris, P. M. Galletti, P. D. Richardson, G. Panol, T. W. Mix, and C. K. Colton.** 1975. A hybrid artificial pancreas. Trans. Am. Soc. Artif. Intern. Organs **21**:8–15.
8. **Cysewski, G. R., and C. R. Wilke.** 1976. Utilization of cellulosic materials through enzymatic hydrolysis. I. Fermentation of hydrolysate to ethanol and single-cell protein. Biotechnol. Bioeng. **18**:1297–1313.
9. **Cysewski, G. R., and C. R. Wilke.** 1977. Rapid ethanol fermentations using vacuum and cell recycle. Biotechnol. Bioeng. **19**:1125–1143.
10. **Davis, J. C.** 1974. Kinetic studies in a continuous steady state hollow fiber membrane enzyme reactor. Biotechnol. Bioeng. **16**:1113–1122.
11. **Del Rosario, E. J., K. J. Lee, and P. L. Rogers.** 1979. Kinetics of alcohol fermentation at high yeast levels. Biotechnol. Bioeng. **21**:1477–1482.
12. **Goldberg, A. L., and J. F. Dice.** 1974. Intracellular protein degradation in mammalian and bacterial cells. Annu. Rev. Biochem. **43**:835–869.
13. **Holzberg, I., R. K. Finn, and K. H. Steinkraus.** 1967. A kinetic study of the alcoholic fermentation of grape juice. Biotechnol. Bioeng. **9**:413–427.
14. **Hunter, K., and A. H. Rose.** 1971. Yeast lipids and membranes, p. 227. *In* A. H. Rose and J. S. Harrison (ed.), The yeasts, vol. 2, Physiology and biochemistry of yeasts. Academic Press, Inc., London.
15. **Jack, T. R., and J. E. Zajic.** 1977. The immobilizaton of whole cells. Adv. Biochem. Eng. **5**:125–145.
16. **Jollow, D., G. M. Kellerman, and A. W. Linnane.** 1968. The biogenesis of mitochondria. III. The lipid composition of aerobically and anaerobically grown *Saccharomyces cerevisiae* as related to the membrane systems of the cells. J. Cell. Biol. **37**:221–230.
17. **Kan, J. K., and M. L. Shuler.** 1978. Urocanic acid production using whole cells immobilized in a hollow fiber reactor. Biotechnol. Bioeng. **20**:217–230.
18. **Kierstan, M., and C. Bucke.** 1977. The immobilization of microbial cells, subcellular organelles, and enzymes in calcium alginate gels. Biotechnol. Bioeng. **19**:387–397.
19. **Knazek, R. A., P. O. Kohler, and P. M. Gullino.** 1974. Hormone production by cells grown *in vitro* on artificial capillaries. Exp. Cell Res. **84**:251–254.
20. **Lightfoot, E. N.** 1974. Transport phenomena and living systems, p. 27. John Wiley & Sons, Inc., New York.
21. **Margaritis, A., and C. R. Wilke.** 1978. The rotorfermentor. II. Application to ethanol fermentation. Biotechnol. Bioeng. **20**:727–753.
22. **Matile, P., H. Moor, and C. F. Robinow.** 1969. Yeast cytology, p. 219–302. *In* A. H. Rose and J. S. Harrison (ed.), The yeasts, vol. 1, Biology of yeasts. Academic Press, Inc., London.
23. **Nagodawithana, T. W., C. Castellano, and K. H. Steinkraus.** 1974. Effect of dissolved oxygen, temperature, initial cell count, and sugar concentration on the viability of *Saccharomyces cerevisiae* in rapid fermentations. Appl. Microbiol. **28**:383–391.
24. **Ramalingham, A., and R. K. Finn.** 1977. The vacuferm process: a new approach to fermentation alcohol. Biotechnol. Bioeng. **19**:583–589.
25. **Reynolds, E. S.** 1963. The use of lead citrate at high pH as an electron-opaque stain in electron microscopy. J. Cell Biol. **17**:208–212.
26. **Rogers, P. L., K. J. Lee, and D. E. Tribe.** 1980. High productivity ethanol fermentations with *Zymomonas mobilis*. Process Biochem. **15**:7–11.
27. **Simpson, K. L., C. O. Chichester, and H. J. Phaff.** 1971. Carotenoid pigments of yeasts, p. 494. *In* A. H. Rose and J. S. Harrison (ed.), The yeasts, vol. 2, Physiology and biochemistry of yeasts. Academic Press, Inc., London.
28. **Spurr, A. R.** 1969. A low-viscosity epoxy resin embedding medium for electron microscopy. J. Ultrastruct. Res. **26**:31–43.
29. **Tze, W. J., and L. M. Chen.** 1977. Long-term survival of adult rat islets of Langerhans in artificial capillary culture units. Diabetes **26**:185–191.
30. **Wada, M., J. Kato, and I. Chibata.** 1980. Continuous production of ethanol using immobilized growing yeast cells. Eur. J. Appl. Microbiol. Biotechnol. **10**:275–287.
31. **Wada, M., J. Kato, and I. Chibata.** 1981. Continuous production of ethanol in high concentration using immobilized growing yeast cells. Eur. J. Appl. Microbiol. Biotechnol. **11**:67–71.
32. **Wallace, P. G., M. Huang, and A. W. Linnane.** 1968. The biogenesis of mitochondria. II. The influence of medium composition on the cytology of anaerobically grown *Saccharomyces cerevisiae*. J. Cell Biol. **37**:207–220.
33. **Waterland, L. R., C. R. Robertson, and A. S. Michaels.** 1975. Enzymatic catalysis using asymmetric hollow fiber membranes. Chem. Eng. Commun. **2**:37–47.
34. **Williams, D., and D. M. Munnecke.** 1981. The production of ethanol by immobilized yeast cells. Biotechnol. Bioeng. **23**:1813–1825.
35. **Winzler, R. J., D. Burk, and V. du Vigneaud.** 1944. Biotin in fermentation, respiration, growth and nitrogen assimilation by yeast. Arch. Biochem. **5**:25–47.
36. **Wolf, C. F. W., and B. E. Munkelt.** 1975. Bilirubin conjugation by an artificial liver composed of cultured cells and synthetic capillaries. Trans. Am. Soc. Artif. Intern. Organs **21**:16–27.
37. **Yarovenko, V. L.** 1978. Theory and practice of continuous cultivation of microorganisms in industrial alcoholic processes. Adv. Biochem. Eng. **9**:1–30.